

Nanoscale Heterogeneity of Polyamide Membranes Formed by Interfacial Polymerization

Viatcheslav Freger*

Ben-Gurion University of the Negev, Laboratory for Desalination and Water Treatment Research, Institutes for Applied Research and Unit of Environmental Engineering, P.O. Box 635, Beer-Sheva 84105, Israel

Received November 18, 2002. In Final Form: March 25, 2003

The nanoscale structure of composite polyamide reverse osmosis (RO) and nanofiltration (NF) membranes was investigated by transmission electron microscopy and atomic force microscopy. The study demonstrated that the polymer density and charge are distributed across the active polyamide layer in a highly nonuniform fashion. The polyamide films appear to be built of a negatively charged outer layer sitting on top of an inner layer possessing a small positive charge. This picture appears to be fairly general for all types of composite membranes and seems to reconcile previously reported contradictory experimental facts concerning measurements of charge for this type of membrane. The sharp boundary between the layers roughly corresponds to the region of the highest polymer density, that is, the actual selective barrier. The location of this barrier deep inside the RO films indicates that formation of the RO polyamide is not limited solely by monomer diffusion through the film, as was suggested previously, but by other factors as well. In the NF polyamide, the location of the boundary nearer toward the surface might suggest a larger role of the diffusion-limited regime in this type of membrane. Comparison of the morphology of standard and high-flux RO membranes showed that the modified procedure used to manufacture the latter apparently results in a more open structure of the active layer, and hence increased surface roughness, and a smaller thickness of the densest barrier. This finding contradicts the currently held view that the high permeability of this type of membrane is a function of increased surface roughness. The results largely support a recently presented theoretical model of polyamide membrane formation via interfacial polymerization.

1. Introduction

Polyamide thin-film composites (TFC) are currently the main type of membrane used in reverse osmosis (RO) and nanofiltration (NF).^{1,2} The dense but thin active layer (skin) of the TFC membrane is formed on top of a microporous support (most often polysulfone) by means of interfacial polymerization (IP).^{3,4} The latter method is also applied in microencapsulation⁵ and in the synthesis of ultrathin polymeric films having responsive and catalytic functions.^{6–8} The technique is based on a polycondensation reaction between two monomers, that is, a polyfunctional amine and an acid chloride, dissolved in immiscible solvents, one of which, the aqueous amine solution, initially impregnates the support. An ultrathin film (skin), well under half a micron thick, is quickly formed at the interface and remains attached to the support. It is commonly believed that the reaction takes place at the organic side of the interface due to the negligible solubility of acid chlorides in water and the fairly good solubility of amines in organic solvents.^{1–4} An additional feature of this method is the possibility of producing membranes possessing fixed charges formed from unreacted amine and (hydrolyzed) acyl chloride

groups. The fixed charges are believed to play a crucial role in the adhesion of foulants and, in NF applications, in selective electrolyte rejection.^{2,9–14}

The extreme thinness of the skin, which is the key to the success of TFC membranes, constitutes a major obstacle to understanding their structure and functioning, since many characterization techniques are not applicable to such thin structures. Recent developments in transport theory in RO and NF membranes have increased the importance of precise knowledge of the characteristics of the skin.^{11–13} Theoretical models have commonly adopted a simplified view of the skin as a uniformly porous or dense film possessing uniformly distributed fixed charge, which has often led to contradictory results.^{11–14}

To date, most of the information on the skin's structure, composition, and charge has been generated using methods developed to probe surfaces. The surface morphology of RO TFC membranes, which has been studied by means of scanning electron microscopy,¹⁵ transmission electron microscopy (TEM),¹⁶ and atomic force microscopy (AFM),^{17–19} has routinely shown a typical rough pattern,

* E-mail: vfreger@bgumail.bgu.ac.il. Phone: +972-8-6479316. Fax: +972-8-6472960.

(1) Cadotte, J. E.; King, R. S.; Majerle, R. J.; Petersen, R. J. *J. Macromol. Sci., Chem.* **1981**, *A15*, 727.
 (2) Petersen, R. J. *J. Membr. Sci.* **1993**, *83*, 81.
 (3) Morgan, P. W. *Condensation Polymers by Interfacial and Solution Methods*; Interscience: New York, 1965.
 (4) Nikonov, V. Z.; Savinov, V. M. In *Interfacial Synthesis*; Millich, F., Carraher, C. R., Jr., Eds.; Marcel Dekker: New York, 1977; Vol. 2.
 (5) Whateley, T. L. In *Microencapsulation: Methods and Industrial Applications*; Benita, S., Ed.; Marcel Dekker: New York, 1996.
 (6) (a) Li, W.; Wamser, C. C. *Langmuir* **1995**, *11*, 4061. (b) Wamser, C. C.; Gilbert, M. I. *Langmuir* **1992**, *8*, 1608.
 (7) Eccleston, M. E.; Slater, N. K. H.; Tighe, B. J. *React. Funct. Polym.* **1999**, *42* (2), 147.

(8) Michalska, Z. M.; Ostaszewski, B.; Zientarska, J. *J. Mol. Catal.* **1989**, *55* (1–3), 256.

(9) Koo, J.-Y.; Petersen, R. J.; Cadotte, J. E. *Polym. Prepr. (Am. Chem. Soc., Div. Polym. Chem.)* **1986**, *27*, 391.

(10) Childress, A.; Elimelech, M. *Environ. Sci. Technol.* **2000**, *34*, 3710.

(11) Yaroshchuk, A. E.; Boiko, Y. P.; Makovetskiy, A. L. *Langmuir* **2002**, *18* (13), 5154.

(12) Hagmeyer, G.; Gimbel, R. *Desalination* **1998**, *117*, 247.

(13) Bowen, W. R.; Welfoot, J. S. *Chem. Eng. Sci.* **2002**, *57*, 1121.

(14) Schaep, J.; Vandecasteele, C.; Mohammad, A. W.; Bowen, W. R. *Sep. Sci. Technol.* **1999**, *34* (15), 3009.

(15) Kwak, S.-Y.; Jung, S. G.; Yoon, Y. S.; Ihm, D. W. *J. Polym. Sci., Part B: Polym. Phys.* **1999**, *37* (13), 1429.

(16) Sundet, S. A. *J. Membr. Sci.* **1993**, *76*, 175.

(17) Kwak, S.-Y.; Jung, S. G.; Yoon, Y. S. *Environ. Sci. Technol.* **2001**, *35* (21), 4334.

with moderate variations of the average roughness between different membranes. An insight into the internal structures of the skin was given by Bartels et al.,²⁰ who used TEM to visualize the cross section of a polyurea TFC membrane prepared by interfacial polymerization of poly-(ethyleneimine) and 2,4-toluene di-isocyanate. It may not be possible, however, to extrapolate some of their conclusions (e.g., that the reaction also occurs partly in the aqueous phase, contrary to the classical mechanism^{1,3,4}) to polyamide films, since the equilibrium partitioning and diffusion between phases of monomers such as poly-(ethyleneimine) seem to be very different from those of the small polyamide monomers. Unfortunately, there are no reports in the literature of TEM studies of polyamide TFC membranes, which could perhaps clarify this point.

The important matter of membrane charge is also subject to controversy. Measurements of the streaming potential along the membrane surface indicate that the polyamide TFC membranes possess significant negative charge.^{10,18,19,21} This agrees with the X-ray photoelectron spectroscopy data^{9,22,23} showing that up to 11% of the acyl chloride groups are not converted to amide. In contrast, attenuated total reflection infrared spectroscopy^{20,22,24} and nuclear magnetic resonance^{9,23} spectroscopy showed only insignificant signals from carboxyls compared to amide groups. Finally, recently reported direct titration experiments revealed the simultaneous presence of both positive and negative fixed charges in the skin layer of composite polyamide NF membranes.²⁵

The essentially nonuniform picture of the skin proposed and analyzed in this paper appears to reconcile these contradictory findings. The work was motivated by the recent theoretical study of interfacial polymerization by Freger and Srebnik,²⁶ who showed that the skin may be expected to be much less homogeneous than is currently believed. On the basis of that theoretical study, we may expect that (i) the fixed charge is not uniform and the skin is actually a "sandwich" comprising two oppositely charged layers and (ii) the polymer density is unevenly distributed over the skin thickness.

In addition, the model suggests that it is the central fraction of the skin's cross section that has the highest density and thus constitutes the selective barrier. These and other essential features revealed by the model will be discussed below, and experimental evidence will be presented for the heterogeneity of the real skin layers of commercial RO and NF TFC membranes based on different polymerization chemistries. Our findings have important implications concerning the mechanism of formation of the skin and the control of its properties.

It will be shown that, despite significant differences in thickness and composition and in agreement with the theoretical picture, the membranes possess remarkable similarity of the inner structure, apparently reminiscent of the IP process. The membrane research community appears to be somewhat unaware of the existence of this "fine structure", presumably because of a certain "resolution gap", that is, certain length scales that have been

largely overlooked in membrane characterization studies. On one hand, methods such as infrared and nuclear magnetic resonance spectroscopy and scanning electron microscopy, with a typical resolution in the micron range, provide information that is averaged over the whole skin. On the other hand, streaming potential and X-ray photoelectron spectroscopy, which are confined to the very small outermost fraction of the skin (of the order of a nanometer), do not shed any light on the internal features. Of the methods suitable for exploring the intermediate range between nanoscopic and microscopic, which is often termed mesoscopic in colloidal science, we have chosen to use TEM. The method is by no means new in the membrane field,^{16,20} but its application to polyamide membranes has been very limited. Our main purpose in the present study was to fill this gap.

2. Experimental Section

2.1. Membranes. The samples studied were high-pressure seawater SWC-1 and high-flux ESPA-1 RO membranes (Hydranautics) and a NF-200 NF membrane (Dow FILMTEC), all kindly supplied by the manufacturers. All were TFC membranes comprising a polyamide skin on top of a porous polysulfone support cast on a polyester nonwoven fabric.

2.2. AFM. Dry membranes were subjected to AFM on an AFM/SPM instrument (Park Scientific), used in the tapping mode, at the Minerva Center, Ben-Gurion University. The average surface roughness was estimated by means of the manufacturer's image processing software.

2.3. TEM. For TEM observations, the polyester backing was peeled off stained (see below) dry samples, so that the porous polysulfone together with the active layer remained. Small pieces were embedded in Araldite resin, and the embedded samples were sectioned with an ultramicrotome into slices 60–90 nm thick. The sections were placed on a carbon/collodion-covered copper grid. TEM images were obtained with a Phillips CM-12 instrument at an accelerating voltage of 120 kV.

Staining of TEM Samples. In unstained samples, the polysulfone support, which contains relatively heavy sulfur atoms, appears considerably darker than the polyamide and may thus be easily distinguished from it. The characteristic porous texture of polysulfone also aids in distinguishing between polyamide and polysulfone. However, only with selective staining may differently charged domains of the polyamide be distinguished from one another. The procedure of Bartels et al.,²⁰ who employed a mixture of uranyl and lead salts to uniformly stain the entire skin, could not be suitable for the present purpose. Since the fixed charges in the skin are those of either the amine or the carboxylic groups, we employed two types of staining, that is, uranyl nitrate to selectively stain the carboxyl-rich regions and sodium tungstate to stain amino groups. The heavy uranyl cations and tungstate anions bind via ion-exchange to the carboxyl and amino groups, respectively. The sodium cations from sodium tungstate could also cause slight darkening of the carboxyl-dominated regions, though not to the same extent. As a result, the contrast between the three regions of interest is somewhat reduced. For uranyl staining, the membranes were treated with 1 mN NaOH solution (to facilitate the subsequent ion-exchange) for 15 min, followed by immersion in 5% uranyl nitrate for about 15 min, thorough washing of the membrane with deionized water in an ultrasonic bath, and drying under a vacuum at 40 °C. For tungstate staining, HCl and sodium tungstate replaced NaOH and uranyl nitrate, respectively. It is likely that small residues of the staining salt solutions could be entrapped or adsorbed in the pores of the polysulfone support, where they would show up as black spots dispersed in the support.

3. Results

3.1. TEM Observations. High-Pressure RO Membrane. Figure 1 shows TEM images of uranyl- and tungstate-stained cross sections of the SWC1 membrane. Figure 1a (uranyl-stained) clearly shows a dark "crust" of about 100–150 nm, apparently the negatively charged part of the

(18) Bowen, W. R.; Doneva, T. A.; Stoton, J. A. G. *Colloids Surf.*, A **2002**, *201*, 73.

(19) Vrijenhoek, E. M.; Hong, S.; Elimelech, M. *J. Membr. Sci.* **2001**, *188*, 115.

(20) (a) Bartels, C. R.; Kreuz, K. L.; Wachtel, A. *J. Membr. Sci.* **1987**, *32*, 291. (b) Bartels, C. R. *J. Membr. Sci.* **1989**, *45* (3), 225.

(21) Ariza, M. J.; Benavente, J.; Rodriguez-Castellon, E.; Palacio, L. *J. Colloid Interface Sci.* **2002**, *247* (1), 149.

(22) Arthur, S. D. *J. Membr. Sci.* **1989**, *46*, 243.

(23) Kwak, S.-Y. *Polymer* **1999**, *40*, 6361.

(24) Freger, V.; Gilron, J.; Belfer, S. *J. Membr. Sci.* **2002**, *209*, 283.

(25) Schaep, J.; Vandecasteele, C. *J. Membr. Sci.* **2001**, *188*, 129.

(26) Freger, V.; Srebnik, S. *J. Appl. Polym. Sci.* **2003**, *88*, 1162.

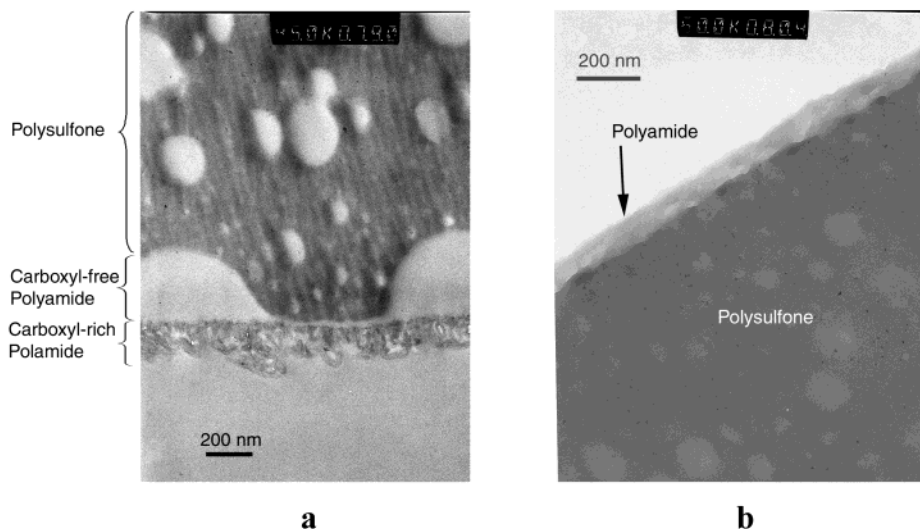


Figure 1. Cross-sectional TEM images of SWC-1 samples: (a) stained with uranyl nitrate, $\times 45\text{K}$; (b) stained with sodium tungstate, $\times 60\text{K}$.

skin sitting on top of a bright positively charged interlayer attached directly to the darker support. The sharp boundary between the differently charged polyamide layers and the irregular polyamide–polysulfone interface is clearly evident.

Figure 1b shows the same membrane treated with tungstate dye. In this case, a brighter polyamide layer of about the same overall thickness as the dark crust in Figure 3a sits on top of a darker underlayer. The boundary between the two is again well-defined and sharp. However, the boundary between the polyamide and polysulfone is hardly discernible due to the insufficient contrast between the (positively charged) interlayer and polysulfone. The lack of contrast in this case presumably results from the relatively low content of free amine groups and, correspondingly, low content of the tungsten atoms, as compared to that of uranium in the stained negatively charged part (cf. Figure 2). Nevertheless, the two images provide good evidence of the existence of the two oppositely charged layers in the polyamide skin.

High-Flux RO Membranes. This class of RO membrane was introduced several years ago by Nitto Denko.²⁷ Patent sources suggest that the manufacturing procedure and chemistry are similar to those for conventional high-flux RO membranes with one important modification: the aqueous phase contains a component whose polarity is intermediate between the polarities of the aqueous phase and the organic phase (e.g., dimethyl sulfoxide or alcohols). The increased flux of these membranes is believed to result from increased roughness and hence increased surface area.^{17,27} Our primary interest was to demonstrate that, with respect to charge distribution, the same interfacial polymerization chemistry produces the same generic type of sandwichlike structure. In addition, we also sought to reveal the internal differences between the two types of RO membrane that could aid understanding of the striking differences in performance between high-pressure and high-flux membranes.

TEM images of uranyl- and tungstate-stained samples of the high-flux membrane show carboxyl-rich and carboxyl-free domains separated by a rather sharp boundary apparently located deep inside the skin (parts a and b of Figure 2, respectively). Inspection of the tungstate-stained micrograph (Figure 2b) shows that, as in Figure 1b, there

is no distinct boundary between the positively charged polyamide and the polysulfone. Yet, at a higher magnification (Figure 2c), an intermediate layer can indeed be observed, despite very poor resolution (presumably, due to excessive thickness of the sample). Contrary to expectations, the dark coloration of the tungstate-stained intermediate layer still appears slightly brighter than both the negatively charged polyamide and the polysulfone.

In contrast to the similarity between the charge distributions for the two types of RO membrane, there were marked morphological differences between the two in terms of the polymer density distribution. Although the overall thickness of the skin was similar for the two types of membrane, that is, about 200–300 nm (excluding the large indentations in the polysulfone support), the structure of the high-flux skin (Figure 2), particularly the carboxyl-rich part, was much more porous and open than that of the high-pressure skin (Figure 1). The former should therefore be much less resistant to water permeation. The truly dense barrier in the high-flux membrane seems to be located only in close proximity to the sharp boundary separating the oppositely charged polyamide layers, whereas for the high-pressure membranes this barrier is apparently much thicker (cf. Figure 1a). Leaving aside the role of the modified procedure in “opening up” the skin structure, which is beyond the scope of the present paper, we postulate that the higher porosity and thinner dense barrier could offer a more realistic explanation for the excellent permeability of the high-flux membranes. This may also account for the slightly lower salt rejection of ESPA-1 versus SWC-1. The increased surface roughness of ESPA-1 should thus be just another consequence of the more open morphology.

Piperazine-Based NF Membranes. TEM micrographs of NF-200 membranes stained with uranyl or tungstate (parts a and b of Figure 3, respectively) show clearly that this membrane is indeed significantly thinner than the RO skin. From Figure 3, we estimate the total thickness of its active layer to be about 20–50 nm versus about 200–300 nm for RO membranes. It is therefore more difficult to distinguish internal features of the skin using TEM in the case of piperazine-based membranes. Nevertheless, despite the large difference in thickness, the fixed charges seem to be distributed across the skin of piperazine- and *m*-phenylenediamine (MPD)-based membranes in a fairly similar fashion. In Figure 3a, a dark

(27) Hirose, M.; Ito, H.; Masatoshi, S.; Tanaka, K. U.S. Patent 5,614,099, 1997.

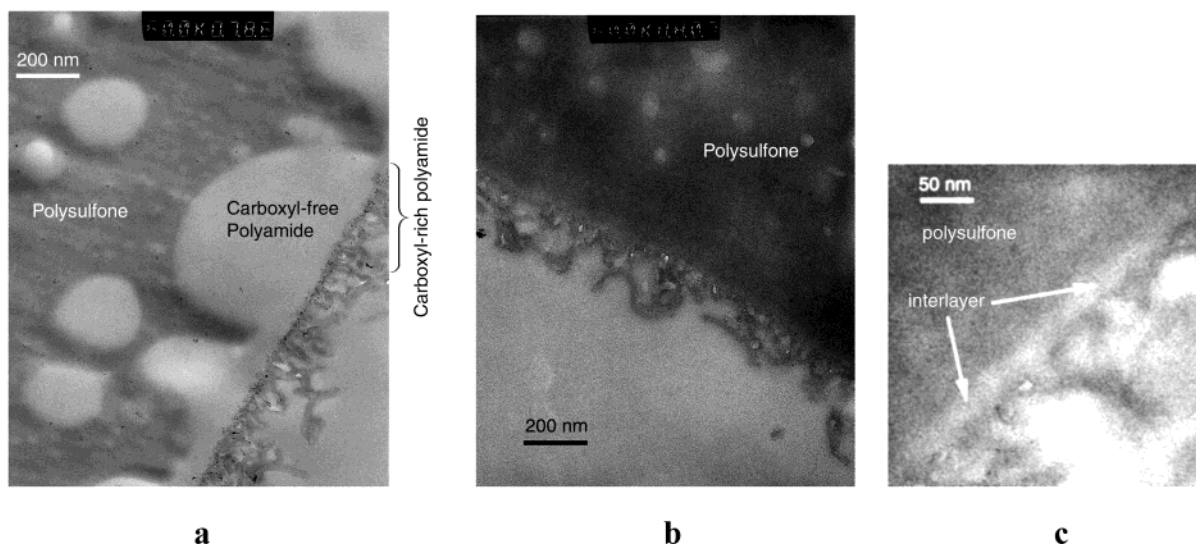


Figure 2. Cross-sectional TEM images of ESPA-1 samples: (a) stained with uranyl nitrate, $\times 60K$; (b) stained with sodium tungstate, $\times 60K$; (c) stained with sodium tungstate, $\times 200K$.

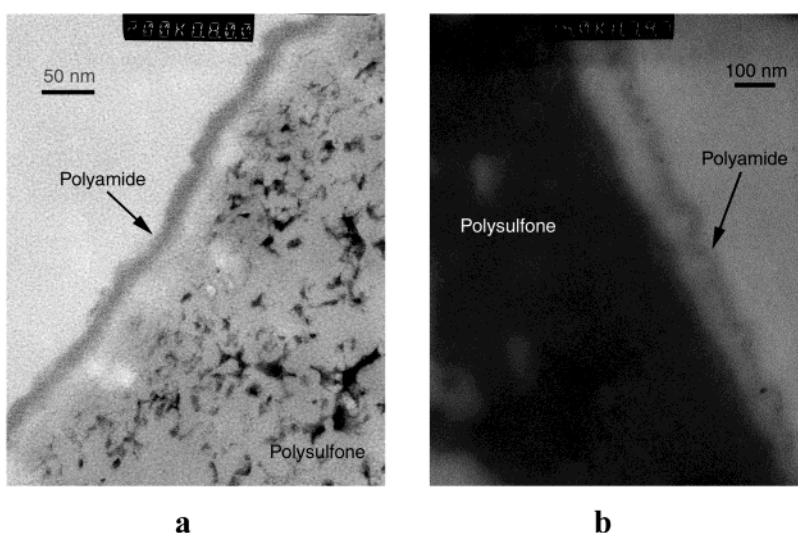


Figure 3. Cross-sectional TEM images of NF-200 samples: (a) stained with uranyl nitrate, $\times 200K$; (b) stained with sodium tungstate, $\times 150K$.

negatively charged layer is clearly visible as is the bright positively charged interlayer. It is evident, however, that the proportion of the bright part in the overall thickness of the skin is notably larger than that for the MPD-based RO membranes. As seen even more clearly than for RO membranes, the tungstate staining changes the relative coloration of differently charged polyamide layers and polysulfone but does not reverse the color sequence, compared to the uranyl staining (Figure 3b). Possible reasons for this finding are discussed below.

3.2. AFM. Figure 4 presents two-dimensional images of the three types of TFC membranes considered in this paper. All membranes are relatively rough, which seems to be a general feature of interfacially polymerized polyamide composite membranes.¹⁶ Potential ways of reducing the surface roughness of TFC membranes and the relationships between surface roughness, synthesis conditions, and membrane performance have been thoroughly scrutinized in numerous publications.^{15–19,24} We therefore wish only to point out two aspects essential in the present context. First, comparison of the average roughness with the minimal thickness of the active layer, as determined from TEM micrographs, shows that the ratio between the two is fairly close to 0.2 for all

membranes, including the thinner (about 15 nm thick) Dow FILMTEC NF-270 NF membrane (not presented here), which suggests that this ratio might represent some intrinsic property of interfacially polymerized polyamide membranes. Second, AFM images once again demonstrate the marked morphological differences between the high-flux and the high-pressure RO membranes, despite their similar average roughness, that is, average height of the protrusions. The protrusions at the surface of the high-pressure RO membrane and of the NF membrane are round, and the surface resembles almost spherical fused particles, whereas the protrusions of the high-flux RO membrane are sharp. Their wormlike sharp-tip shape is also clearly visible in the TEM images presented in Figure 2.

4. Discussion

An in-depth interpretation of the results must take into consideration the theoretical Freger–Srebnik (FS) model of interfacial polymerization²⁶ mentioned briefly in the Introduction. Previous models of interfacial polymerization considered formation of the film (assumed uniform) to be a diffusion-limited process, i.e., a steady increase in thickness starting from zero thickness, whereby amine

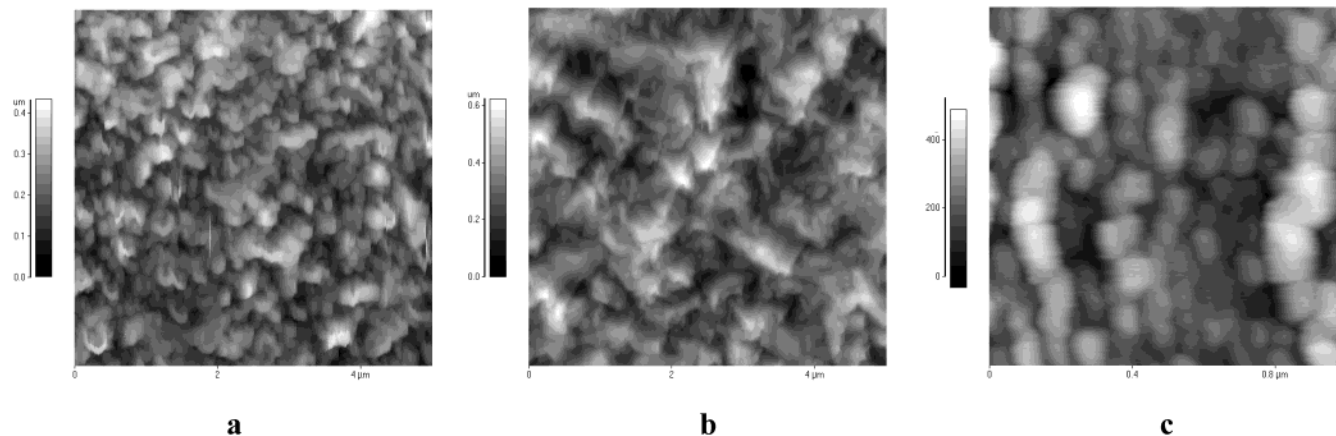


Figure 4. AFM images of dry membranes: (a) SWC-1, image size $5 \times 5 \mu\text{m}$; (b) ESPA-1, image size $5 \times 5 \mu\text{m}$; (c) NF-200, image size $1 \times 1 \mu\text{m}$.

diffuses to the other side of the film where it immediately reacts with the acyl chloride, which is assumed to be completely excluded from the film.^{28–31} On the assumption that there are no interfering effects (e.g., limited supply of amine³¹ or competing hydrolysis reaction²⁸) and a quasi-steady-state amine profile across the skin, the following relationship may be written:²⁹

$$\delta = (2D_p C_a t)^{1/2} \quad (1)$$

where δ is the film thickness at elapsed time t , D_p is the permeability of the film to the amine, and C_a is the amine concentration. Equation 1 has shown good agreement with the growth of some polyamide films at long reaction times.^{29,31} However, in the case of the films used in TFC membranes two objections may be raised concerning the assumptions made for eq 1. First, zero initial thickness implies infinitely fast diffusion, and thus the reaction, however fast, cannot be regarded as instantaneous during some finite initial period. Second, the monomers that are used in membrane manufacturing have been chosen to form a film that is almost impermeable to anything but water; that is, D_p in eq 1 would be very low. This suggests that the film formed during the initial period is likely to seal the interface and largely inhibit the subsequent “standard” diffusion-limited growth described by eq 1.

To take these points in account, the FS model²⁶ does not make any assumptions about the structure of the film during the interfacial polymerization process. Instead, it attempts to explicitly obtain this structure by solving equations of diffusion and reaction in the organic boundary layer adjacent to the interface for the five relevant species: two monomers, a polymer, and two types of reactive end groups of the polymer. The basic conclusion that followed from the simulations was that the structure of the TFC membrane skin is determined primarily by the incipient film that forms throughout a finite reaction zone during the initial period. It is the thickness of this incipient film that ultimately determines the thickness of the mature film. As illustrated in Figures 5 and 6, this has profound consequences on the kinetics of the process and film structure and their dependence on the kinetic

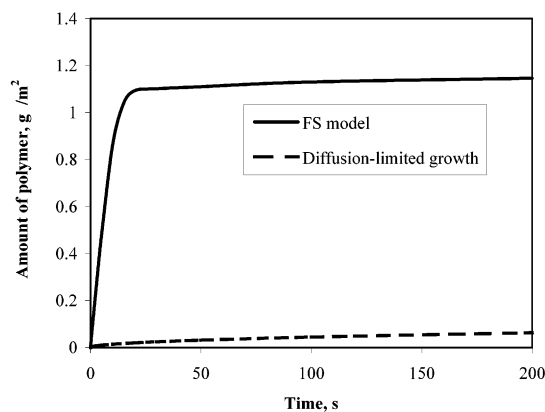


Figure 5. Typical kinetics of polymer formation in the course of interfacial polymerization between a bifunctional amine and trifunctional acyl chloride calculated using the FS model (ref 26), with the following parameters (see eqs 1 and 2): $C_a = 0.01\%$ (corresponding to 1% concentration in water and a distribution coefficient of 100), $C_b = 0.1\%$, $L = 20 \mu\text{m}$, reactivity of functional groups for monomer–monomer and monomer–polymer reactions $k_r = k/f_a f_b = 10^5 \text{ L}/(\text{mol}\cdot\text{s})$, for polymer–polymer reaction $k_p = 0.01 k_r$, bulk diffusivity of monomers $D = 10^{-9} \text{ m}^2/\text{s}$; amine permeability through dense polyamide $D_p = 10^{-4} D$. For comparison, the kinetics for simple diffusion-limited growth is also shown (the same C_a and D_p , instant reaction, and a linear quasi-steady-state concentration profile of amine across the growing film are assumed).

parameters and synthesis conditions, which may be summarized as follows.

(1) The thickness δ of the reaction zone and hence that of the incipient film may be given approximately by the following scaling relationship:²⁶

$$\delta \sim \left[\frac{LD}{k(C_a f_a + C_b f_b)} \right]^{1/3} \quad (2)$$

where C_a is the equilibrium concentration of the amine at the organic side of the interface, C_b is the acyl chloride concentration in the organic phase, L is the thickness of the diffusion boundary layer at the interface (estimated to be of the order of 10^{-5} m), D is the diffusivity of the monomers in the organic phase, k is the rate constant of the bimolecular reaction between the two monomers, and f_i is the functionality of monomer i . In contrast to eq 1, eq 2 suggests that δ decreases slowly with an increase in the concentration of either monomer. However, the subsequent diffusion-limited growth may eventually reverse this trend, particularly for very high amine concentrations

(28) (a) Enkelman, V.; Wegner, G. *Makromol. Chem.* **1976**, *177*, 3177. (b) Enkelman, V.; Wegner, G. *Appl. Polym. Symp.* **1976**, *26*, 5365.

(29) Jansen, L. J. J. M.; te Nijenhuis, K. *J. Membr. Sci.* **1992**, *65*, 59.

(30) Karode, S. K.; Kulkarni, S. S.; Suresh, A. K.; Mashelkar, R. A. *Chem. Eng. Sci.* **1997**, *52*, 3243.

(31) Ji, J.; Dickson, J. M.; Childs, R. F.; McCarry, B. E. *Macromolecules* **2000**, *33*, 624.

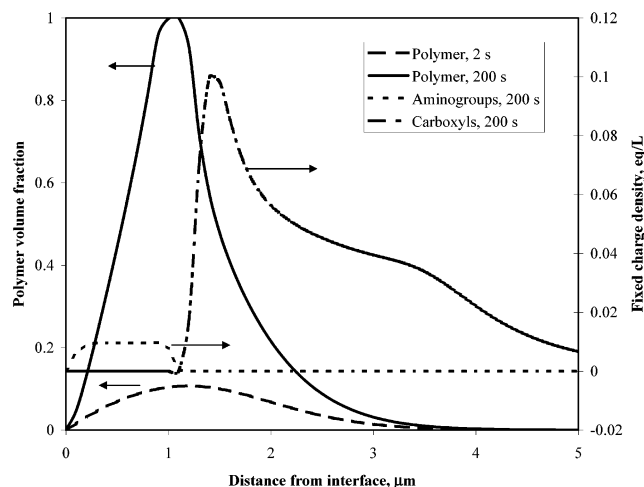


Figure 6. Calculated concentration profiles of polymer (at 2 and 200 s elapsed time) and of amine and acyl chloride groups after 200 s. The parameters used are the same as those in Figure 5.

(see eq 1 and Figure 5). Chai and Krantz³² did indeed observe a shallow minimum in the dependence of thickness on the amine concentration.

(2) As long as the polymer does not cause a strong reduction of the bulk diffusivity inside the reaction zone, its thickness and location remain fairly constant (cf. the polymer density profiles at 2 and 200 s in Figure 6), as does the rate of polymer formation. This rate is determined by the diffusivity of monomers across the polymer-free boundary layer, rather than by the much slower diffusion through the polymer film. As a result, a film of finite thickness is formed rapidly, followed by an abrupt slowdown of the interfacial polymerization process (Figure 5), a finding that agrees much better than eq 1 with the kinetic study of Chai and Krantz³² and with actual manufacturing experience.¹

(3) Equation 1 does not contain the reaction constant k . The FS model explicitly predicts that the film thickness scales as $k^{-1/3}$, which agrees with the fact that MPD (the RO monomer, $k \sim 10^2\text{--}10^3 \text{ L}\cdot\text{mol}^{-1}\cdot\text{s}^{-1}$)⁴ produces films of about an order of magnitude thicker than films of piperazine (a popular NF monomer, $k \sim 10^4\text{--}10^5$)⁴ and an order of magnitude thinner than sulfamide films ($k < 0.1$).³² The difference in thickness between the RO and NF membranes used in this study is therefore to be expected.

(4) The polymer density across the film is not uniform and shows a dense core hidden inside a looser polymer (Figure 6). Presumably, the dense core constitutes the water-selective barrier, which is therefore significantly thinner than the superficial thickness of the polyamide, particularly in high-flux RO membranes.

(5) The fixed charge of the membrane is negative at the outer surface and positive at the other side of the film. Besides, the positive and negative domains have rather different charge concentrations (the negative part contains more fixed charges) and are separated by a sharp boundary located inside the densest part of the skin, as illustrated in Figure 6.

The asymmetric nature of polyamide films formed by interfacial polymerization has previously been reported,^{6,27–32} yet little indication has been given as to how deep the domains extend into the film. The diffusion-limited growth model stipulates that the entire film, save

the thinnest outmost fraction, should be amine dominated, that is, it should possess a positive fixed charge. The FS model suggests that in the initial period the sharp boundary between the oppositely charged domains should pass much deeper inside the film.

It should be stressed that the FS model includes the slow diffusion-limited regime that takes place once the reaction zone has become filled with polymer, as indicated by the plateau in Figure 5. Nevertheless, this slow stage needs to last a relatively long time for it to cause any significant morphological change. It thus seems reasonable to assume that the thickness and morphology of the film might be shaped, to a large extent, by the initial period of polymer formation. In principle, any of the interrelated features (1) to (5) could serve as an indication of the dominance of the initial period of formation. As indicated above, the first three are actually supported by experimental facts, but for the last two no evidence has been found so far.

Returning now to Figures 1 and 2, we conclude that the significant thickness of the negatively charged layer and the inner location of the boundary between the negatively and positively charged domains apparently demonstrate that the process of polyamide formation in RO membranes could not advance into the truly diffusion-limited regime.

The weak coloration of the positively charged interlayer after tungstate staining (Figures 1–3) might be a manifestation of the very low fixed charge (free amine content) in this layer, in agreement with the simulations (see the fixed charge density profiles in Figure 6). Yet, it could also be explained by a lower density of polyamide in the layer. It has been postulated that the film actually forms at some distance from the interface.^{1,3,4} This is clearly evident in the simulated density profile in Figure 6 and suggests that the amine-dominated interlayer (or a part of it) may be quite loose and thus appear brighter in the TEM micrograph, even when stained.

It is quite obvious from Figure 1 and, particularly, from Figure 2 that not the whole RO skin serves as a selective barrier but rather a small central fraction that is perfectly dense and contains no pores. This finding is in good agreement with the theoretical picture drawn from the FS model, which once again suggests that film formation actually stops after this barrier has been created and no further film densification (pore filling) occurs. However, there is no evidence that this is also true for the NF film, since the whole NF film looks fairly dense (Figure 3).

The larger proportion of the positively charged part in the overall thickness of the piperazine membrane (Figures 1 and 3) might indicate that in this case the interfacial polymerization process has advanced significantly more into the diffusion-limited stage than in the case of RO films. NF membranes are known to be more permeable than RO polyamides,^{2,33} and the initially formed thin film could allow slow further growth that might eventually push the negatively charged layer somewhat farther away from the support and increase the thickness of the amine-dominated carboxyl-free part. Although this has important implications for the kinetics of film formation, it still does not change our basic conclusion about the characteristic fixed charge heterogeneity of the three types of membranes investigated here.

A theoretical explanation of the characteristic rough surface morphology of the polyamide TFC membranes revealed by AFM (Figure 4) presents a serious challenge

(32) Chai, G.-Y.; Krantz, W. B. *J. Membr. Sci.* **1994**, *93*, 175.

(33) Linder, C.; Kedem, O. In *Nanofiltration Principles and Applications*; Schaefer, A. I., Fane, A. G., Waite, T. D., Eds.; Elsevier: New York, 2002.

to future modeling efforts for the interfacial polymerization process, since roughness is perhaps the most important feature that the FS model, as well as all previous models, cannot handle. The fundamental reason is that they all are of the mean-field type, that is, all local variables (e.g., concentrations) are smoothed, while the source of roughness apparently lies in large local fluctuations of these variables at the polyamide–organic solvent interface. Using an oversimplified approach, we could try to relate the roughness to the thickness of the loose fringes of the bell-like profile of the polymer density (Figure 1b). This loose part of the film could irregularly precipitate onto the densest part afterward and give rise to the rough morphology. It seems to correlate well with the above observation that the ratio of average roughness to thickness is fairly constant for various samples. However, arguments presented by Sundet,¹⁶ based on ultra-small-angle X-ray scattering results, suggest that fluctuations leading to particle formation at various scales could occur throughout the entire active layer during interfacial polymerization and not only on the polyamide surface. This emphasizes the complexity of the interfacial polymerization process and suggests that more complete models will inevitably have to go beyond the simple mean-field approximation.

5. Conclusions

The TEM observations show very reasonable agreement with the new theoretical picture and indicate that the real polyamide composite membranes used in RO and NF are by no means homogeneous structures characterized by a single value of parameters such as charge or local polymer density. Such membranes seem to possess a double-layer structure, in which the outmost negatively charged layer is separated from the porous support by a

dense intermediate positively charged layer of lower absolute charge. It is likely that this feature will generally be found in polyamide composite membranes prepared by the interfacial polymerization method.

Nevertheless, some differences were observed among the various types of membrane: piperazine-based and MPD-based membranes differed significantly in terms of thickness, in agreement with the theoretical predictions based on the higher reactivity of piperazine. Similarly, the negatively charged part of the NF skin seems somewhat thinner than that in other membranes, indicating that the conventional diffusion-limited regime might play some role in the formation of NF, but not RO, films.

High-flux RO membranes synthesized using a modified procedure show, on average, a higher porosity and a much thinner dense barrier than the standard high-pressure RO membrane. The latter finding offers a more plausible explanation for the increased flux of these membranes than the earlier assumed increased surface roughness.

The prediction of roughness in general and explanations for its variation with different chemistries and synthetic conditions cannot be properly analyzed in terms of the available models. This presents a challenge for future theoretical work.

Acknowledgment. The help of Dr. Ronit Popovitz-Biro (Weizmann Institute of Science, Rehovot, Israel) in performing the TEM analyses and of Ms. Roxana Golan and Mr. Juergen Jopp of the Minerva Center, Ben-Gurion University of the Negev, for AFM measurements is gratefully acknowledged. The author also thanks Professor Ora Kedem and Dr. Charles Linder for valuable comments.

LA020920Q